Inorganic Chemistry
Article

Inorg. Chem. **2009**, *48*, 5269–5278 **5269**
DOI: 10.1021/ic9002065

Synthesis of Lithium *N*-pentafluorophenyl, *N′*-trimethylsilyl 2-Pyridylamidinate and Its Cyclization to Lithium Tetrafluoro-2-(2-pyridyl)benzimidazolate via a Me_3SiF Elimination. Coordination Chemistry, Reactivity, and Mechanism

Sinai Aharonovich, Mark Botoshanski, and Moris S. Eisen*

Schulich Faculty of Chemistry and Institute of Catalysis Science and Technology, Kyriat Hatechnion, Haifa, 32000, Israel

Received February 3, 2009

When *N*-trimethylsilylpentafluoro aniline reacts with BuLi in the presence of THF or TMEDA, the corresponding THF (**2**) or TMEDA (**4**) lithium anilides are obtained. Complex **4** is monomeric in the solid state, with a distorted trigonal pyramidal coordination geometry at the lithium center. The strong C−F→Li interaction in this complex is also accompanied by the elongation of the C−F bond. Mild heating of complex **4** with 2-cyanopyridine results in rapid evolution of Me_3SiF to quantitatively yield the tetrafluoro-2-(2-pyridyl)benzimidazolate lithium complex (**6**). From the reaction mixture of complex **4** the asymmetric *N*-trimethylsilyl, *N′*-pentafluorophenyl-2-pyridylamidinate lithium complex (**5**) was isolated as a dormant intermediate. Complex **5** possesses several unusual bonding features with the most notably being a very short Si−N bond length and a rare κ^1-Z-syn amidinate bonding mode. A mechanism that includes silicon assisted C−F bond activation is proposed for the cyclization reaction based on the structural parameters of complexes **5** and **6**, and on ^{1}H, ^{19}F, and ^{13}C NMR studies.

Introduction

The synthesis of group IV complexes with ligands that have predetermined characteristics for their use as catalysts in a variety of chemical transformations, such as olefin polymerization and other olefin related processes, is an important goal with many potential returns in organometallic chemistry.[1] One of the advantages of utilizing amidinates, $[N(R_1)C(R_2)N(R_3)]^-$, well-known as ancillary ligands in coordinative chemistry,[2−4] is the possibility to rationally affect their properties through choice of the carbon and nitrogen substituent.[3,5−9] In the design of improved amidinate ligands we took note of the dramatic affect on the catalytic behavior of the well-known Phi (phenoxy imine) catalysts, when the nitrogen substituent was replaced from a phenyl to a pentafluorophenyl group.[10,11] We especially focused on the ability of the fluorine atom close enough to the active catalytic metal center to suppress the termination pathway and furnished a "living" polymerization catalyst.[11] A conceptual question regards the generality of such interaction and whether similar introduction of a fluoroaryl moieties on an amidinate nitrogen would generate similar desired outcomes.[12] Putting the β-H elimination processes at bay, the other nitrogen and carbon substituents of the ligand can be designed to promote the activity and reactivity of the metal center, providing an adequate steric protection and decreasing the donor ability of the NCN backbone. The second nitrogen substituent was therefore chosen to be $SiMe_3$, since its introduction to the

*To whom correspondence should be addressed. E-mail: chmoris@tx.technion.ac.il.

(1) For selected recent reviews, see: (a) Matsugi, T.; Fujita, T. *Chem. Soc. Rev.* **2008**, *37*, 1264–1277. (b) Domski, G. J.; Rose, J. M.; Coates, G. W.; Bolig, A. D.; Brookhart, M. *Prog. Polym. Sci.* **2007**, *32*, 30–92. (c) Prashar, S.; Antinolo, A.; Otero, A. *Coord. Chem. Rev.* **2006**, *250*, 133–154. (d) Wang, B. *Coord. Chem. Rev.* **2006**, *250*, 242–258. (e) Mueller, T. E.; Hultzsch, K. C.; Yus, M.; Foubelo, F.; Tada, M. *Chem. Rev.* **2008**, *108*, 3795–3892. (f) Smolensky, E.; Eisen, M. S. *J. Chem. Soc., Dalton Trans.* **2007**, 5623–5650.

(2) Edelmann, F. T. *Coord. Chem. Rev.* **1994**, *137*, 403–481.

(3) Junk, P. C.; Cole, M. L. *Chem. Commun.* **2007**, 1579–1590.

(4) (a) Kissounko, D. A.; Zabalov, M. V.; Brusova, G. P.; Lemenovskii, D. A. *Russ. Chem. Rev.* **2006**, *75*, 351–374. (b) Schareina, T.; Kempe, R. Amido ligands in coordination chemistry. In *Synthetic methods of organometallic and inorganic chemistry*; Herrmann, W. A., Ed.; Thieme: Germany, **2002**; Vol. *10*, pp 1−41.

(5) Baker, R. J.; Jones, C. *J. Organomet. Chem.* **2006**, *691*, 65–71.

(6) Knapp, C.; Lork, E.; Watson, P. G.; Mews, R. *Inorg. Chem.* **2002**, *41*, 2014–2025.

(7) Volkis, V.; Nelkenbaum, E.; Lisovskii, A.; Hasson, G.; Semiat, R.; Kapon, M.; Botoshansky, M.; Eishen, Y.; Eisen, M. S. *J. Am. Chem. Soc.* **2003**, *125*, 2179–2194.

(8) Schmidt, J. A. R.; Arnold, J. *J. Chem. Soc., Dalton Trans.* **2002**, 3454–3461.

(9) (a) Schmidt, J. A. R.; Arnold, J. *J. Chem. Soc., Dalton Trans.* **2002**, 2890–2899. (b) Nimitsiriwat, N.; Gibson, V. C.; Marshall, E. L. Takolpuckdee, P.; Tomov, A. K.; White, A. J. P.; Williams, D. J.; Elsegood, M. R. J.; Dale, S. H. *Inorg. Chem.* **2007**, *46*, 9988–9997.

(10) (a) Sakuma, A.; Weiser, M.-S.; Fujita, T. *Polym. J.* **2007**, *39*, 193–207. (b) Furuyama, R.; Saito, J.; Ishii, S.; Makio, H.; Mitani, M.; Tanaka, H.; Fujita, T. *J. Organomet. Chem.* **2005**, *690*, 4398–4413.

(11) Makio, H.; Fujita, T. *Bull. Chem. Soc. Jpn.* **2005**, *78*, 52–66.

(12) Xie, G.; Qian, C. *J. Polym. Sci. A: Polym. Chem.* **2007**, *46*, 211–217.

Published on Web 05/18/2009

amidinate system would attribute steric bulk and lower nucleophilicity of the nitrogen and increased solubility of the complex in non-polar solvents.[8] Another advantage of the TMS moiety is the ability to harness the tendency of the trimethylsilyl group for facile 1,3 sigmatropic shifts,[13,14] which enable the use of readily available nitriles and *N*-silylated lithium amides as starting materials in their corresponding syntheses.[6,15−17] As for the central carbon, its substitution with electron withdrawing groups will increase the polymerization activity, as demonstrated by titanium[18] and vanadium[19] pentafluorophenyl amidinates. We have recently shown that the use of heterocyclic motifs as the carbon substituents promotes the catalytic activity of the resulting complexes in the polymerization of α-olefins.[20] Lithium amidinate complexes, besides their prominent use as ligand transfer reagents in the preparation of amidinates of p-, d-, and f-block elements[2,7,8,21] are also important reagents and\or intermediates in various organic syntheses such as the preparation of 1,3,5-triazapentadienes,[22] 1,3,5 triazines,[7,23] bicyclic thia-aza heterocycles,[24] 7-azaindole,[25] benzimidazoles,[26] and in the coupling of alkynes and carbodiimides.[27] In this presentation we disclose the synthesis of various fluorinated lithium complexes, their unique structure, and their reactivity which leads to facile, room temperature, and atom efficient one pot route toward the tetrafluorinated lithium benzimidazolate $LiC_6F_4N_2C(2\text{-}C_5H_4N)$, in quantitative yields. Benzimidazolates, along with the free base benzimidazoles, are an important class of compounds having very rich coordinative chemistry.[28] Benzimidazoles serve as ligands of cobalt in vitamin B_{12}[29] and also have widespread pharmacological activities[30,31] such as antihypertensive,[32] antitumor,[33] anti-inflammatory,[34] antiparasitic,[31,33,35,36] antiviral,[33,37] antifungal,[38] antimicrobial,[31,33,39] and gastric acid suppressant[31,36,40] drugs.

Scheme 1. Synthetic Route for the Silylated Pentafluoroanilide Lithium Complexes **2**−**4**

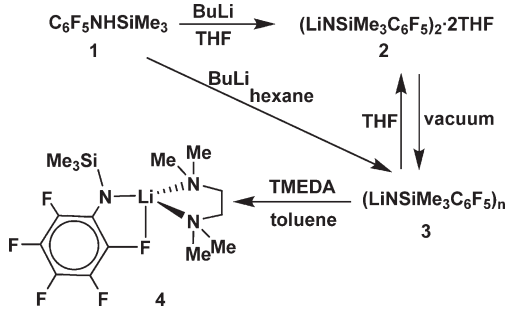

Results and Discussion

Preparation and Reactivity of the Lithium Amides. Deprotonation of *N*-trimethylsilyl pentafluoroaniline (**1**) with BuLi proceeds rapidly above −10 °C, giving a clear solution of the amide THF adduct **2** in THF or a white precipitate of the corresponding lithium amide **3** in hexane (Scheme 1). Removal of all the THF solvent from complex **2** by vacuum afforded the lithium amide **3**. Addition of THF to the white powder of complex **3** at −78 °C is exothermic, producing complex **2**. Addition of TMEDA (TMEDA = *N*,*N*,*N*′,*N*′-tetramethylethylenediamine) to a toluene suspension of **3** yields a yellow-tan solution from which faint-yellow crystals of the lithium-TMEDA amide adduct **4** can be isolated.

Caution should be exercised when THF is added to dry powder of complex **3**. When the addition is carried out at room temperature a spontaneous combustion is observed

(13) (a) Schaumann, E.; Kirschning, A. *Synlett* **2007**, 177–190. (b) Makita, K.; Koketsu, J.; Ando, F.; Ninomiya, Y.; Koga, N. *J. Am. Chem. Soc*. **1998**, *120*, 5764–5770. (c) Takahashi, M.; Kira, M. *J. Am. Chem. Soc*. **1999**, *121*, 8597–8603.
(14) Kira, M.; Iwamoto, T. *Chemistry of Organic Silicon Compounds*; Rappoport, Z., Apeloig, Y., Eds.; John Wiley & Sons: Chichester, U.K., **2001**; Vol. *3*, pp 853−948.
(15) Aharonovich, S.; Kapon, M.; Botoshanski, M.; Eisen, M. S. *Organometallics* **2008**, *27*, 1869–1877.
(16) Lisovskii, A.; Botoshansky, M.; Eisen, M. S. *J. Chem. Soc., Dalton Trans*. **2001**, 1692–1698.
(17) (a) Antolini, F.; Hitchcock, P. B.; Khvostov, A. V.; Lappert, M. F. *Can. J. Chem*. **2006**, *84*, 269–276. (b) Eisen, M. S.; Kapon, M. *J. Chem. Soc., Dalton Trans*. **1994**, 3507–3510. (c) Lee, H. K.; Lam, T. S.; Lam, C.-K.; Li, H.-W.; Fung, S. M. *New J. Chem*. **2003**, *27*, 1310–1318.
(18) Liguori, D.; Centore, R.; Tuzi, A.; Grisi, F.; Sessa, I.; Zambelli, A. *Macromolecules* **2003**, *36*, 5451–5458.
(19) Brussee, E. A. C.; Meetsma, A.; Hessen, B.; Teuben, J. H. *Chem. Commun*. **2000**, 497–498.
(20) Aharonovich, S.; Kapon, M.; Botoshanski, M.; Eisen, M. S. Substituent Effects in Propylene Polymerization Promoted by Titanium(IV) Amidinates. Proceedings of the 38th International Conference on Coordination Chemistry, Kenes International, Jerusalem, Israel, July 20−25 **2008**; p 369.
(21) For selected recent examples and reviews, see: (a) Green, S. P.; Jones, C.; Jin, G.; Stasch, A. *Inorg. Chem*. **2007**, *46*, 8–10. (c) Lisovskii, A.; Eisen, M. S. *Top. Organomet. Chem*. **2005**, *10*, 63–105. (d) Nagashima, H.; Kondo, H.; Hayashida, T.; Yamaguchi, Y.; Gondo, M.; Masuda, S.; Miyazaki, K.; Matsubara, K.; Kirchner, K. *Coord. Chem. Rev*. **2003**, *245*, 177–190. (e) So, C.-W.; Roesky, H. W.; Magull, J.; Oswald, R. B. *Angew. Chem., Int. Ed*. **2006**, *45*, 3948–3950. (f) Wilder, C. B.; Reitfort, L. L.; Abboud, K. A.; McElwee-White, L. *Inorg. Chem*. **2006**, *45*, 263–268.
(22) Boesveld, W. M.; Hitchcock, P. B.; Lappert, M. F. *J. Chem. Soc., Dalton Trans*. **1999**, 4041–4046.
(23) Boesveld, W. M.; Hitchcock, P. B.; Lappert, M. F. *J. Chem. Soc., Perkin Trans*. **2001**, *1*, 1103–1108.
(24) Knapp, C.; Lork, E.; Borrmann, T.; Stohrer, W.-D.; Mews, R. *Eur. J. Inorg. Chem*. **2003**, 3211–3220.
(25) Ma, Y.; Breslin, S.; Keresztes, I.; Lobkovsky, E.; Collum, D. B. *J. Org. Chem*. **2008**, *73*, 9610–9618.
(26) Inukai, Y.; Oono, Y.; Sonoda, T.; Kobayashi, H. *Bull. Chem. Soc. Jpn*. **1979**, *52*, 516–520.
(27) Ong, T.-G.; O'Brien, J. S.; Korobkov, I.; Richeson, D. S. *Organometallics* **2006**, *25*, 4728–4730.
(28) For recent reviews, see: (a) Tellez, F.; Lopez-Sandoval, H. Castillo-Blum, S. E.; Barba-Behrens, N. *ARKIVOC* **2008**, *5*, 245–275. (b) Lyaskovskyy, V. V.; Voitenko, Z. V.; Kovtunenko, V. A. *Chem. Heterocycl. Compd*. **2007**, *43*, 253–276. (c) Chan, W. K. *Coord. Chem. Rev*. **2007**, *251*, 2104–2118. (d) Luneau, D.; Rey, P. *Chem. Heterocycl. Compd*. **2005**, *249*, 2591–2611.
(29) Krautler, B. Cobalt B_{12} Enzymes and Coenzymes. In *Encyclopedia of Inorganic Chemistry*, 2nd ed.; King, R. B., Ed.; John Wiley & Sons: Chichester, U.K., **2005**; Vol. *2*, pp 345−365.
(30) (a) Spasov, A. A.; Yozhitsa, I. N.; Bugaeva, L. I.; Anisimova, V. A. *Pharm. Chem. J*. **1999**, *33*, 232–243. (b) Joshi, K. C.; Jain, R.; Dandia, A.; Sharma, K. *J. Fluorine Chem*. **1992**, *56*, 1–27.
(31) Bhattacharya, S.; Chaudhuri, P. *Curr. Med. Chem*. **2008**, *15*, 1762–1777.
(32) Yagupolskii, L. M.; Maletina, I. I.; Petko, K. I.; Fedyuk, D. V.; Handrock, R.; Shavaran, S. S.; Klebanov, B. M.; Herzig, S. *J. Fluorine Chem*. **2001**, *109*, 87–94.
(33) Boiani, M.; Gonzalez, M. *Coord. Chem. Rev*. **2005**, *5*, 409–424.
(34) Sondhi, S. M.; Singhal, N.; Johar, M.; Reddy, B. S. N.; Lown, J. W. *Curr. Med. Chem*. **2002**, *9*, 1045–1074.
(35) Keiser, J.; Engels, D.; Buescher, G.; Utzinger, J. *Expert Opin. Invest. Drugs* **2005**, *14*, 1513–1526.
(36) Velik, J.; Baliharova, V.; Fink-Gremmels, J.; Bull, S.; Lamka, J.; Skalova, L. *Res. Vet. Sci*. **2004**, *76*, 95–108.
(37) De Clercq, E.; Naesens, L. *J. Clin. Virol*. **2006**, *37*, S82–S86.
(38) (a) Didier, E. S.; Maddry, J. A.; Brindley, P. J.; Stovall, M. E.; Didier, P. J. *Expert Rev. Anti-Infect. Ther*. **2005**, *3*, 419–434.
(39) Muri, E. M. F.; Williamson, J. S. *Mini-Rev. Med. Chem*. **2004**, *4*, 201–206.
(40) Sharara, A. I. *Expert Rev. Anti-Infect. Ther*. **2005**, *3*, 863–870.

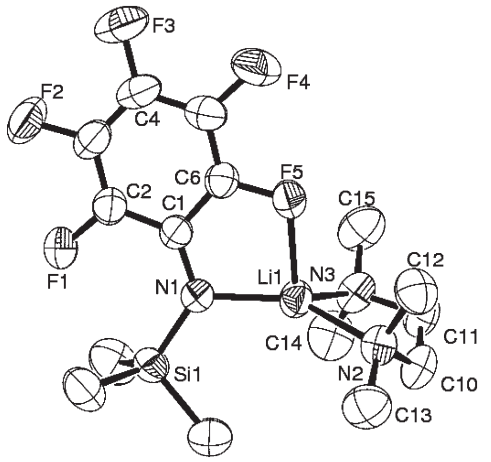

Figure 1. ORTEP illustration of the molecular structure of complex **4** (50% thermal ellipsoids). Hydrogen atoms are omitted for clarity.

even under argon atmosphere. The violent decomposition of complex **3** under these conditions, which is accompanied by formation of LiF, is probably helped by the exothermic solvation of **3** by THF.

Structure of $LiNTMSC_6F_5 \cdot TMEDA$. In the solid state complex **4** (Figure 1) is mononuclear with the lithium atom being tetracoordinated and chelated by TMEDA and by the N1−C1−C6−F5 motif. Crystallographic data and structure refinement details for complex **4** and selected bond lengths and angles are collected in Tables 1 and 2, respectively. The predominantly sp^2 hybridized anilide nitrogen N1 (sum of angles around N1 = 359.93°) is σ bonded to the lithium atom as indicated by the coplanarity of the metal and the aromatic ring, and by the short C1−N1 bond length of 1.351 Å.[41,42] The short distance of the Li atom from the plane (0.241 Å), formed by the anilide nitrogen N1 and the two TMEDA nitrogen atoms N2 and N3, indicates that the lithium atom adopts a slight distorted trigonal pyramid, with the lithium at the center of its base while the fluorine atom occupies the apical position. This uncommon lithium coordination environment can be seen as a midway structure between the trigonal lithium in $LiN(SiMe_3)_2 \cdot TMEDA$[43] and the trigonal bipyramide of $[LiN(C_6F_5)_2 \cdot THF]_2$[44] and $LiN(C_6F_5)SiMe_2F \cdot 2THF$[45] in which two fluorine atoms occupy the corresponding axial positions. The strong Li←F−C interaction in **4** is evident from the short Li−F distance (2.082 Å), which practically equals the sum of the ionic radius of the metal and the van der Waals radius of fluorine.[46]

Interestingly, this strong Li−F interaction is accompanied by elongation of the C−F bond by 0.025 Å as compared to the non-interacting *ortho* or *para* C−F bonds. Similar M···F−C cation-dipole attractions between aromatic and aliphatic fluorocarbons and Lewis acidic s-block metals have been reported in the literature.[46,47]

Comparison of the ^{1}H NMR spectra of the neutral aniline **1** and the lithium anilides of compounds **2** and **4**, at room temperature, revealed that in all cases the TMS signal is split to a triplet with a small coupling constant (J = 1.5, 1.3, and 1.4 Hz for **1**, **2**, and **4**, respectively). This coupling is the result of a through-space interaction between the TMS hydrogen atoms and the *ortho*-ring fluorine atoms.[48] The identical interaction of the two *ortho* fluorine atoms in solution at room temperature in anilides **2** and **4** indicates that similar to other lithium fluoroanilides[44,45,49] the Li−F interaction is very labile.

Reaction of the Complex 4 with 2-Cyano Pyridine. Following the well-established protocol for the preparation of silylated amidinates from amides and nitriles,[2,7,15,16] 2-cyano pyridine was added to a cold solution of the amido complex **4**, and the reaction mixture was stirred for 96 h (Scheme 2).

Surprisingly, ^{1}H and ^{19}F NMR spectra showed that the crude reaction mixture was composed of almost exclusively two products: the amidinate **5**, as a minor component (ca. ∼30% yield) and the benzimidazolate complex **6** as the major component (ca. ∼70% yield) (vide infra). To gain an insight into the course of this reaction, we have followed it by ^{1}H and ^{19}F NMR spectroscopy (Figure 2).

When the reaction was stopped after 2 h, analytically pure crystals of the amidinate **5**, suitable for X-ray diffraction studies were isolated by slow evaporation of the solvent. The ^{1}H and ^{19}F NMR spectra of solution of complex **5** (which is stable in the solid state) in C_7D_8 were measured 10 min after its preparation and 96 h later. Comparison of the change of the ^{1}H and ^{19}F NMR spectra in time shows that the consumption of the amidinate **5** and the appearance of the benzimidazolate **6** are accompanied by formation of Me_3SiF, which appears as a doublet in the ^{1}H NMR spectrum and as a multiplet in the ^{19}F spectrum owing to the coupling $^3J_{F-H}$ = 7.2 Hz (Figure 2, spectra i and ii).[50] Comparison of the ^{19}F NMR spectra (iv) and (v) of complex **6** (Figure 2) shows that while the signals of the pure compound appear as a wide singlet, the same signals in the reaction mixture are split ($^3J_{F-F}$ = 17.5 Hz, albeit small changes in the chemical shift are observed). These differences in the signal shape indicate that the presence of complex **5** changes the solution behavior of complex **6**, caused presumably by interactions of the fluorine atoms with the lithium metal.[45] Hence, TMSF can be ruled out as the major interacting species because of the apparent splitting of the fluorine resonance.

The clean and slow room temperature conversion of complex **5** to complex **6** and the lower solubility of the

(41) Allen, F. H.; Kennard, O.; Watson, D. G.; Brammer, L.; Orpen, A. G.; Taylor, R. *J. Chem. Soc., Perkin Trans. 2* **1987**, S1−S19.
(42) (a) von Buelow, R.; Gornitzka, H.; Kottke, T.; Stalke, D. *Chem. Commun.* **1996**, 1639–1640. (b) von Bilow, R.; Deuerlein, S.; Stey, T. Herbst-Irmer, R.; Gornitzka, H.; Stalke, D. *Z. Naturforsch., B: Chem.* **2004**, *59*, 1471–1479.
(43) Henderson, K. W.; Dorigo, A. E.; Liu, Q.-Y.; Williard, P. G. *J. Am. Chem. Soc.* **1997**, *119*, 11855–11863.
(44) Khvorost, A.; Shutov, P. L.; Harms, K.; Lorberth, J.; Sundermeyer, J.; Karlov, S. S.; Zaitseva, G. S. *Z. Anorg. Allg. Chem.* **2004**, *630*, 885–889.
(45) Stalke, D.; Klingebiel, U.; Sheldrick, G. M. *Chem. Ber.* **1988**, *121*, 1457–1459.
(46) Plenio, H. *Chem. Rev.* **1997**, *97*, 3363–3384.
(47) (a) Shmulinson, M.; Pilz, A.; Eisen, M. S. *J. Chem. Soc., Dalton Trans.* **1997**, 2483–2486. (b) Barrett, A. G. M.; Crimmin, M. R.; Hill, M. S.; Hitchcock, P. B.; Procopiou, P. A. *Angew. Chem., Int. Ed.* **2007**, *46*, 6339–6342. (c) Abe, T.; Tao, G.-H.; Joo, Y.-H.; Huang, Y.; Twamley, B.; Shreeve, J. n. M. *Angew. Chem., Int. Ed.* **2008**, *47*, 7087–7090. (d) Plenio, H. *ChemBioChem* **2004**, *5*, 650–655.
(48) Oliver, A. J.; Graham, W. A. G. *J. Organomet. Chem.* **1969**, *19*, 17–27.
(49) Lee, W.-Y.; Liang, L.-C. *Inorg. Chem.* **2008**, *47*, 3298–3306.
(50) Schmidbaur, H. *J. Am. Chem. Soc.* **1963**, *85*, 2336–2337.

Table 1. Crystallographic Data for Complexes **4**−**6**

	complex **4**	complex **5**	complex **6**
empirical formula	$C_{15}H_{25}F_5LiN_3Si$	$C_{21}H_{27}F_5LiN_5Si$	$C_{18}H_{18}F_4LiN_5$
Fw[g/mol]	377.41	479.51	387.31
T[K]	240(2)	240(2)	240(1)
λ[Å]	0.71073	0.71073	0.71073
crystal system	monoclinic	monoclinic	monoclinic
space group	$C2/c$	$P2_1/c$	$P2_1/c$
a[Å]	19.258(4)	10.987(2)	12.897(2)
b[Å]	7.2770(10)	17.479(3)	11.960(2)
c[Å]	28.944(6)	14.737(3)	12.980(3)
β[deg.]	100.71(3)	113.47(3)	106.45(3)
V[Å^3]	3985.6(13)	2596.0(8)	1920.2(6)
Z	8	4	4
ρ[g/cm^3]	1.258	1.227	1.340
μ(Mo Kα)[mm^{-1}]	0.164	0.143	0.109
R1, wR2 ($I > 2\sigma(I)$)	0.0592, 0.1875	0.0677, 0.1635	0.0516, 0.1401
R1, wR2 (all data)	0.0791, 0.1956	0.1854, 0.2017	0.0881, 0.1576
GOF on F^2	1.120	0.900	0.996
F(000)	1584	1000	800
θ range for data collection [deg.]	2.80 to 25.43	1.90 to 25.00	2.36 to 25.33
limiting indices	$0 \le h \le 23$	$0 \le h \le 12$	$0 \le h \le 15$
	$0 \le k \le 8$	$-20 \le k \le 0$	$0 \le k \le 14$
	$-34 \le l \le 34$	$-17 \le l \le 15$	$-15 \le l \le 14$
reflections collected/unique	12442/3566	16194/4357	12523/3488
	[R(int) = 0.0580]	[R(int) = 0.0890]	[R(int) = 0.0490]
completeness to θ_{max} [%]	96.60	95.50	99.20
data/restraints/parameters	3566/0/233	4357/0/298	3488/0/273
largest diff. peak and hole [e/Å^{-3}]	0.216 and −0.172	0.231 and −0.189	0.199 and −0.205

Table 2. Key Bond Lengths [Å] and Angles [deg] for Complex **4**

bond lengths		bond and dihedral angles	
N(1)−Li(1)	1.961(5)	N(1)−Li(1)−N(2)	139.8(3)
N(2)−Li(1)	2.099(6)	N(1)−Li(1)−N(3)	128.1(3)
N(3)−Li(1)	2.108(6)	N(2)−Li(1)−N(3)	87.4(2)
F(5)−Li(1)	2.082(5)	F(5)−Li(1)−N(1)	83.9(2)
C(6)−F(5)	1.374(3)	F(5)−Li(1)−N(2)	106.8(2)
C(2)−F(1)	1.349(4)	F(5)−Li(1)−N(3)	104.9(2)
C(4)−F(3)	1.348(4)	C(6)−F(5)−Li(1)	107.8(2)
C(1)−N(1)	1.351(3)	C(1)−N(1)−Li(1)	110.0(2)
Si(1)−N(1)	1.706(2)	C(1)−N(1)−Si(1)	128.48(19)
		Li(1)−N(1)−C(1)−C(6)	8.23

latter in toluene can be utilized to obtain large single crystals of **6** by keeping a concentrated toluene solution of **5** undisturbed for 2 weeks. When a toluene solution of complex **5** is heated to 50 °C its conversion to complex **6** is completed in less than 10 min, accompanied by a rapid and massive bubbling of TMSF. The conversion of the amidinate **5** to the benzimidazolate **6** in a closed vessel is not accompanied by LiF elimination to form the silylated amidine or the benzimidazole (Scheme 2), although the reaction of TMSF with various C,[51] N,[52] and O[53] nucleophiles is known in the literature.

Solid State Structure of the Lithium Amidinate Complex 5. Crystallographic data and structure refinement details for complex **5** and selected bond lengths and angles are collected in Tables 1 and 3, respectively. The solid state structure of **5** (Figure 3) is non habitual in several regards. The tetrahedral lithium atom is chelated by a TMEDA molecule and a NCCN fragment; the latter consist of the pentafluoroanilide and the pyridyl nitrogens. Comparison of the structures of complex **5** and [(2-C_5H_4N)C($NSiMe_3$)$_2$]Li·TMEDA[15] reveals that the substitution of one TMS group on the nitrogen with the sterically similar C_6F_5 group[54] changes the metal-amidinate coordination mode (κ^1 and κ^2, respectively). The κ^1 coordination in complex **5** therefore stems mainly from electronic effects.

The geometry of the amidinate moiety in complex **5** exhibits the *Z-syn* tautomer (Scheme 3), rarely observed in anionic amidinates.[3,5] The *syn* conformation can be rationalized by the preference of the lithium atom for chelation by the four atom N2−C1−C2−N1 unit. The favorable bonding of the hard lithium center with the sp^2 orbital of the pyridine nitrogen dictates the near planarity of the Li−N−C−C−N metallacycle. This in turn places the TMS group attached to the nitrogen N5 between two hard choices in purely steric hindrance terms; in most aryl amidinates the aromatic ring on the central carbon is nearly perpendicular to the amidinate backbone, leaving enough space to the nitrogen substituents (in this case the TMS group), which results in the widely observed *E* tautomers.

In complex **5** the pyridyl ring is locked in the co-planar position, which will put the TMS group in the E isomer in close proximity to the pyridyl ring. The second alternative, the *Z* tautomer, situates the TMS group in close proximity to the C_6F_5 ring, which unlike the pyridyl ring can rotate to relieve some of the steric hindrance, as indeed indicated by the dihedral angle between the amidinate and the C_6F_5 groups (74.8 °). Interestingly, atoms

(51) (a) Cunico, R. F. *Tetrahedron Lett*. **1986**, *27*, 4269–4272. (b) Della, E. W.; Tsanaktsidis, J. *Organometallics* **1988**, *7*, 1178–1182. (c) Hitchcock, P. B.; Lappert, M. F.; Leung, W.-P.; Liu, D.-S.; Mak, T. C. W.; Wang, Z.-X. *J. Chem. Soc., Dalton Trans*. **1999**, 1257–1262.

(52) (a) Fredelake, B.; Ebker, C.; Klingebiel, U.; Noltemeyer, M.; Schmatz, S. *J. Fluorine Chem*. **2004**, *125*, 1007–1017. (b) Klingebiel, U.; Noltemeyer, M.; Wand, A. *J. Organomet. Chem*. **2006**, *691*, 2657–2665. (c) Matthes, C.; Noltemeyer, M.; Klingebiel, U.; Schmatz, S. *Organometallics* **2007**, *26*, 838–845.

(53) Schuette, S.; Freire-Erdbruegger, C.; Klingebiel, U.; Sheldrick, G. M. *Phosphorus, Sulfur Silicon Relat. Elem*. **1993**, *78*, 75–81.

(54) Hansch, C.; Leo, A.; Hoekman, D. *Exploring QSAR: Hydrophobic, Electronic, and Steric Constants*; American Chemical Society: Washington, DC, **1995**; pp 254−270.

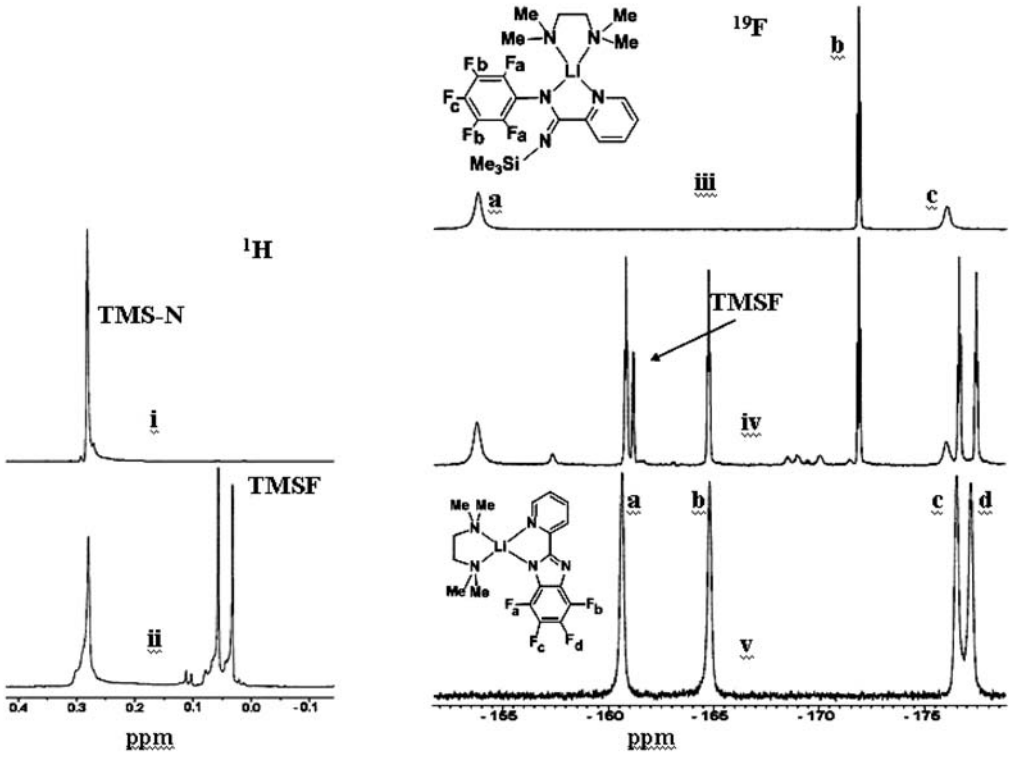

Figure 2. ^{1}H and ^{19}F NMR follow up of the reaction of amidinate complex **5** to benzimidazolate **6**. ^{1}H NMR spectra of the TMS region of (i) freshly prepared sample of **5** and (ii) the same sample after 96 h. ^{19}F NMR spectra of (iii) the freshly prepared sample of **5**, (iv) the same sample after 96 h, and (v) the analytically pure compound **6**.

Scheme 2. Synthesis of Lithium Tetrafluorobenzimidazolate (**6**) via the Amidinate Intermediate (**5**)

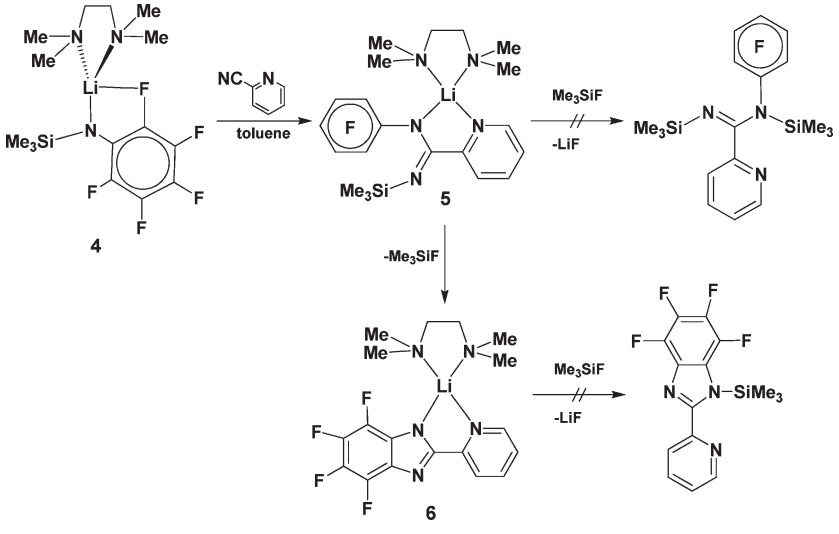

C7, C8, and Si from the TMS group are parallel and equidistant to the C21, C17, and C16 atoms of the C_6F_5 ring, respectively. While the C···C contact distances are slightly larger than their van der Waals radii,[56] the C16···Si1 distance (3.513 Å) is 0.287 Å shorter than the sum of their van der Waals radii,[56] suggesting that a plausible interaction between silicon and the π system of the ring is operative. Interestingly, the C1−C2 bond length (1.510 Å) in complex **5** is identical to the analogous bond in the complex $[(2\text{-}C_5H_4N)C(NSiMe_3)_2]Li\cdot TMEDA$.[15] The near perpendicularity of the NCN moiety and the pyridyl ring in the latter imply that there is no major charge delocalization among these moieties in complex **5**. The two C−N bonds are not equivalent with C1−N2 and C1−N5 bond lengths of 1.343 and 1.289 Å respectively, which are out of the average range (1.315−1.330 Å ± 0.006) found for this bond in 12 bis *N*-silylated aryl amidinates.[15] Particularly unusual is the bonding of the silicon. The Si1−N5 bond length of 1.663 Å ± 0.003 is

(55) The nomenclature of the amidinate isomers/tautomers is adopted from: Patai, S.; Rappoport, Z. *The chemistry of amidines and imidates*; Wiley: Chichester, U.K., **1991**.

(56) Bondi, A. *J. Phys. Chem. A* **1964**, *68*, 441–451.

Table 3. Key Bond Lengths [Å], Angles [deg], and Contact Distances [Å] for Complex **5**

bond lengths		bond and dihedral angles		contact distances	
N(1)−Li(1)	2.034(8)	N(1)−Li(1)−N(2)	83.0(3)	C(7)···C(21)	3.463
N(2)−Li(1)	1.977(7)	N(1)−Li(1)−N(3)	118.6(4)	Si(1)···C(16)	3.513
N(3)−Li(1)	2.086(9)	N(2)−Li(1)−N(3)	121.4(4)	C(8)···C(17)	3.510
N(4)−Li(1)	2.071(9)	N(4)−Li(1)−N(1)	120.4(4)		
C(1)−N(2)	1.343(5)	N(4)−Li(1)−N(2)	131.0(4)		
N(2)−C(16)	1.392(5)	N(4)−Li(1)−N(3)	86.6(3)		
Si(1)−N(5)	1.663(3)	Li(1)−N(1)−C(2)−C(1)	0.5		
C(1)−N(5)	1.290(5)	C(1)−N(2)−C(16)	116.9(3)		
C(1)−C(2)	1.510(5)	C(1)−N(2)−C(16)−C(17)	74.8		
		Si(1)−N(5)−C(1)	150.9(3)		
		N(5)−C(1)−N(2)	131.8(4)		
		N(5)−C(1)−C(2)	116.4(4)		
		N(5)−C(1)−C(2)−C(3)	4.5		
		Li(1)−N(2)−C(1)−C(2)	7.5		

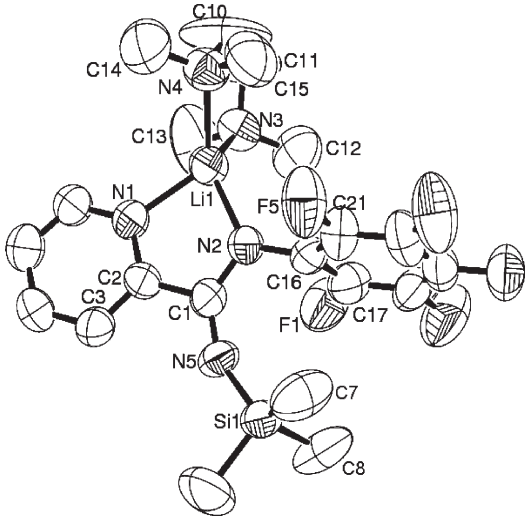

Figure 3. ORTEP diagram of the molecular structure of complex **5** (50% thermal ellipsoids). Hydrogen atoms are omitted for clarity.

Scheme 3. Structures and Accepted Nomenclatures of the Amidinate Tautomeric Forms[55]

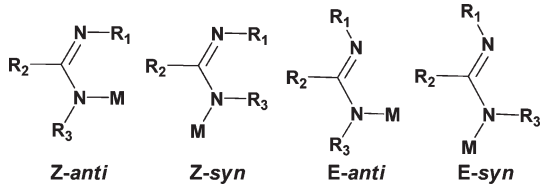

evidently shorter in comparison to the average *N*-$SiMe_3$ length in the aforementioned silylated amidinates (1.703 Å ± 0.005), and to the best of our knowledge is among the shortest Si−N bonds observed in tetra-coordinated silicon compounds with tri carbon substituents. This short Si−N bond indicates that electron density is donated from N5 to the Si atom. The formation of this partial Si···N bond is also corroborated by the Si1−N5−C1 angle of 150.9 ± 0.3.

Solid State Structure of the Lithium Benzimidazolate Complex 6. Crystallographic data and structure refinement details for complex **6** and selected bond lengths and angles are collected in Tables 1 and 4, respectively.

In complex **6**, the lithium metal has a tetrahedral geometry, and it is chelated by the TMEDA and the NCCN unit of the 2-(2-pyridyl) tetrafluorobenzimidazolate ligand

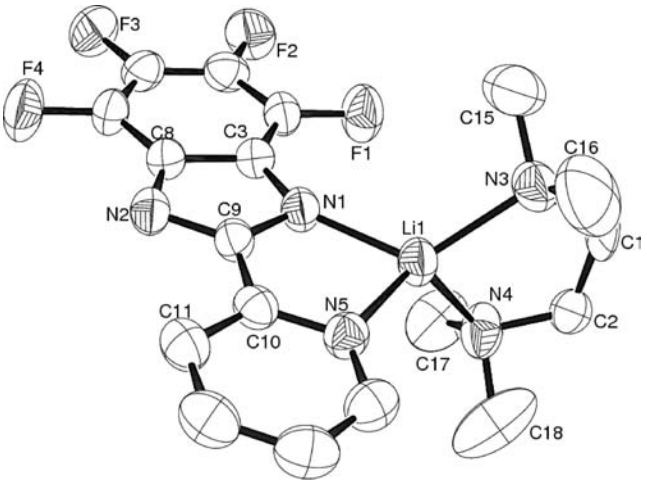

Figure 4. ORTEP diagram of the molecular structure of complex **6** (50% thermal ellipsoids). Hydrogen atoms are omitted for clarity.

Table 4. Key Bond Lengths [Å] and Angles [deg] and for Complex **6**

bond lengths		bond and dihedral angles	
N(1)−Li(1)	1.978(4)	N(4)−Li(1)−N(3)	88.51(16)
N(4)−Li(1)	2.085(4)	N(1)−Li(1)−N(3)	124.0 (2)
N(3)−Li(1)	2.074(4)	N(5)−Li(1)−N(3)	125.05(19)
N(5)−Li(1)	2.081(4)	N(5)−Li(1)−N(4)	119.14(19)
N(1)−C(9)	1.361(3)	N(1)−Li(1)−N(4)	119.58(19)
N(1)−C(3)	1.362(3)	N(1)−Li(1)−N(5)	84.51(15)
N(2)−C(9)	1.341(3)	N(1)−C(9)−C(10)	119.82(18)
N(2)−C(8)	1.369(3)	N(1)−C(9)−N(2)	117.40(19)
C(10)−C(9)	1.462(3)	N(2)−C(9)−C(10)	122.74(19)
		C(9)−N(2)−C(8)	101.99(17)
		C(9)−N(1)−C(3)	102.22(17)
		N(1)−C(9)−N(2)−C(8)	0.26
		N(1)−C(9)−C(10)−N(5)	2.02
		C(9)−N(2)−C(8)−C(7)	0.21
		Li(1)−N(1)−C(9)−C(10)	0.98
		Li(1)−N(5)−C(10)−C(9)	3.69

(Figure 4). The C−N bond lengths in the imidazole ring fall in the range of 1.341−1.369 Å, which are typical of pyroles.[41] Comparison of the structures of **5** and **6**, which have a very similar steric environment near the lithium metal, shows that in the latter, the electron density is partially donated from the pyridyl ring to the perfluorobenzimidazolate π system, as indicated by the shortening of the C9−C10 bond length (1.462 Å ± 0.003), as compared to its counterpart in complex **5** (C1−C2 = 1.510 Å ± 0.005; Figure 3). It seems that this electron donation

Scheme 4. Plausible Three-Step Cyclization Mechanism[a]

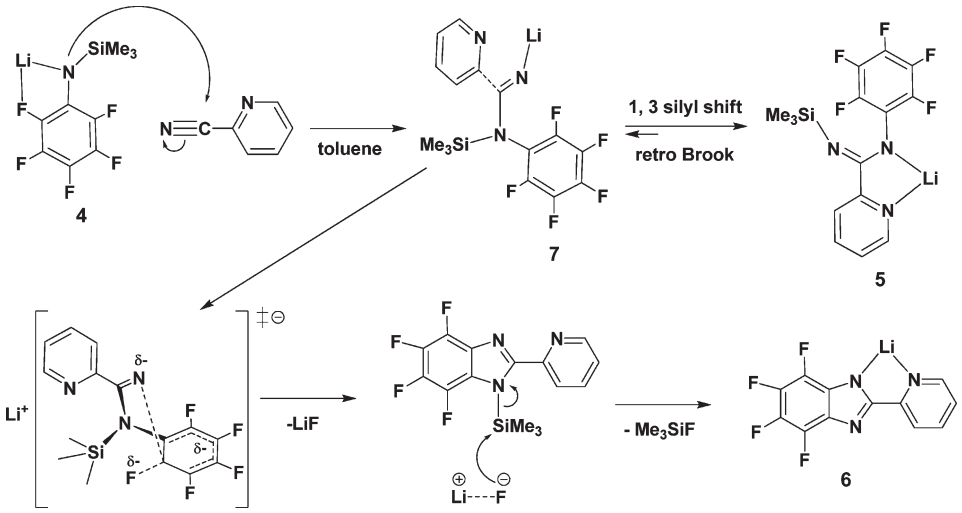

[a] Option *i*, see text; the TMEDA ligand at the lithium atom was omitted for clarity.

reduces the Lewis basicity of the pyridyl nitrogen, as evident from the elongation of the $Li-N_{py}$ bond from 2.034 Å ± 0.008 in complex **5** to 2.081 Å ± 0.004 in complex **6**. This electron donation is also corroborated by the ^{13}C NMR spectrum of complex **6**, which exhibits a downfield shift for the resonance of the methine carbon adjacent to the pyridyl nitrogen (155.57 ppm in **6**; 145.31 ppm in **5**). In solution and at room temperature the solid state structure of **6** is retained, as indicated by the four different ^{19}F NMR signals (Figure 2(v)).

Mechanistic Insights into the Cyclization of the Amidinate 5 toward the Corresponding Benzimidazolate Complex 6. Three potential mechanisms are conceivable for the cyclization reaction of the amidinate compound **5** into the benzimidazolate complex **6**.

(i) A three-step mechanism, which first includes a 1,3 retro-brook rearrangement [14,57] of the amidinate **5** to the imide **7** (Scheme 4). The latter complex participates in a nucleophilic aromatic attack on the *ortho* carbon of the C_6F_5 ring,[58] followed by a concomitant nucleophilic attack of the fluoride ion on the silicon to yield TMSF and the benzimidazolate **6**.

(ii) A "four-centered" transition state σ-bond metathesis mechanism (Figure 5) involving the *ortho* C−F bond of the C_6F_5 moiety and the Me_3Si-N moiety in complex **5**.[59]

(iii) A two-step silicon-assisted nucleophilic aromatic substitution.[60] In the first step the imide complex **7** is obtained as described above (option i), and in the second step the Lewis acidic silicon participates in a concerted silicon-assisted nucleophilic attack of the imido nitrogen on the *ortho* carbon of the C_6F_5 moiety with the formation of a twisted-boat-like six-membered ring transition state (**9**). Complex **9** can either eliminate a TMSF molecule as part of the concerted mechanism or form a hypervalent silicon adduct **8** that can eliminate TMSF to form complex **6**[61] (Scheme 5).

On the basis of the solid state structures of the complexes and their ^1H and ^{19}F NMR spectra in solution, we propose the third option as the major operative mechanism. In the proposed mechanism (i), the nucleophilic attack was already suggested for the cyclization of *N*-pentafluorophenylamidines to benzimidazole under basic conditions.[26] This reaction proceeds only at elevated temperatures, after prolonged reaction times, and in a polar solvent (DMF), as often observed in other nucleophilic aromatic substitution reactions.[62]

Since in many fluoro aryl compounds the rate determining step (RDS) in a nucleophilic attack is the C−F bond cleavage, [58] the cyclization observed in our hands (room temperature) of the silylated amidinate **5**, hints that the activation of the C−F bond by silicon is likely to be the main factor lowering the activation barrier for the intramolecular nucleophilic attack.

In the second σ bond metathesis mechanism (ii), the four-centered transition state will result in a highly twisted four-membered ring with a poor overlap among the orbitals. This geometry configuration is expected to proceed, if operative, only at high temperatures, whereas for complex **5** the reaction occurs as already mentioned even without heating.

In the third proposed mechanism, silicon-assisted nucleophilic aromatic substitution (iii), the amidinate complex **5** is in equilibrium with the imido complex **7**. Interestingly, this equilibrium can be corroborated via ^1H NMR (room temperature) showing a nice singlet

(57) (a) Moser, W. H. *Tetrahedron* **2001**, *57*, 2065–2084. (b) Kleinfeld, S. H.; Wegelius, E.; Hoppe, D. *Helv. Chim. Acta* **1999**, *82*, 2413–2424. (c) Shaviv, E.; Botoshansky, M.; Eisen, M. S. *J. Organomet. Chem.* **2003**, *683*, 165–180.

(58) O'Hagan, D. *Chem. Soc. Rev.* **2008**, *37*, 308–319.

(59) (a) Jarvie, A. W. P. *Organomet. Chem. Rev.* **1970**, *6*, 153–207. (b) Sommer, L. H. *Stereochemistry, mechanism and silicon*; McGraw-Hill: New York **1965**. (c) Chuiko, A. A.; Lobanov, V. V.; Grebenyuk, A. G. Structure of disperse silica surfaces and electrostatic aspects of adsorption. In *Colloidal Silica*; Bergna, H. E., Roberts, W. O., Eds.; CRC Press: Boca Raton, FL, **2006**; pp 331−360.

(60) (a) Douvris, C.; Ozerov, O. V. *Science* **2008**, *321*, 1188–1190. (b) Yadav, V. K.; Balamurugan, R. *Org. Lett.* **2001**, *3*, 2717–2719.

(61) Sakurai, H. Silicon: Organosilicon Chemistry. In *Encyclopedia of Inorganic Chemistry*, 2nd ed.; King, R. B., Ed.; John Wiley & Sons: Chichester, U.K., **2005**; Vol. *2*.

(62) Carey, F. A. *Organic Chemistry*, 4th ed.; McGraw-Hill: Boston, **2000**; pp 917−933.

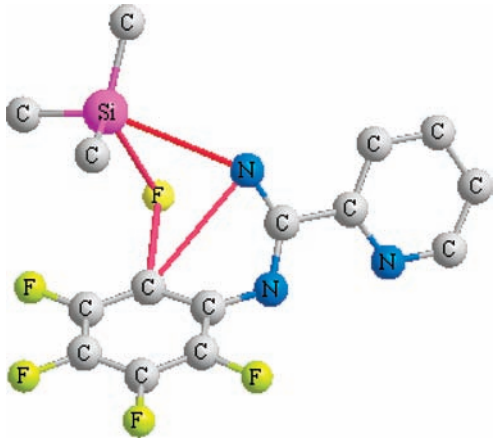

Figure 5. CemBio3D schematic representation of the four-centered transition state in the σ bond metathesis mechanism (ii), showing that if operative, a highly puckered four-membered ring Si−F−C−N transition state is acquired (the dihedral angle F−Si−N−C = 62 °). For clarity, the four relevant σ bonds are colored in red (Li·TMEDA moiety was omitted for clarity).

signal for the TMS group of complex **5** and a small triplet (J_{F-H} = 1.4 Hz) of the TMS group of the imido complex **7** (Figure 6(i)). Important to point out that the TMS triplet signal of the starting lithium amido **4** appears at a different chemical shift with the same coupling constant.

Upon the intramolecular nucleophilic aromatic substitution in complex **7**, the silicon coordinates to the partially negatively charged fluorine from the polarized C−F bond. The collapse of the σ-complex **9** to give TMSF and the benzimidazolate **6** can be achieved in one or two steps (Scheme 5). The presence of a coordinated TMSF (preferentially as described in complex **8**) is supported by the presence of a broad small singlet in the ^{1}H NMR spectrum at 0.011 ppm (Figures 6), 0.03 ppm upfield from the chemical shift of uncoordinated TMSF (Figures 2(ii) and 6(ii)). The assignment of this signal to the silicate **8** is corroborated by an independent experiment in which TMSF was added to a solution of pure complex **6**. The TMS region of the ^{1}H NMR spectrum of this mixture shows, besides the expected large doublet of the unreacted TMSF, a small signal at the *same chemical shift* (compare Figures 6(i) and 6(ii)). The lack of an observable splitting (broadening is noticed) of this signal due to the vicinal $^3J_{F-H}$ coupling is known in the literature for similar hypervalent silicates.[63]

The fact that complex **5** can be isolated, indicates that the rate of the 1,3 silyl sigmatropic shift is much faster than that of the relevant nucleophilic attack, and therefore **5** can be described as the "dormant" species only at low temperatures.

Studies on the scope of this reaction toward various fluoro benzimidazolates, as well as the coordination chemistry and reactivity of the tetrafluorobenzimidazolate ligands to form group IV metal complexes, are currently underway.

(63) (a) Breliere, C.; Carre, F.; Corriu, R. J. P.; Douglas, W. E.; Poirier, M.; Royo, G.; Wong Chi Man, M. *Organometallics* **1992**, *11*, 1586–1593. (b) Cho, H. M.; Jang, J. I.; Kim, C. H.; Lee, S.-G.; Lee, M. E. *J. Organomet. Chem.* **2003**, *679*, 43–47. (c) Kalikhman, I.; Gostevskii, B.; Kingston, V.; Krivonos, S.; Stalke, D.; Walfort, B.; Kottke, T.; Kocher, N.; Kost, D. *Organometallics* **2004**, *23*, 4828–4835.

Scheme 5. Plausible Silicon-Assisted Nucleophilic Attack Mechanism for the Formation of Complex **6**[a]

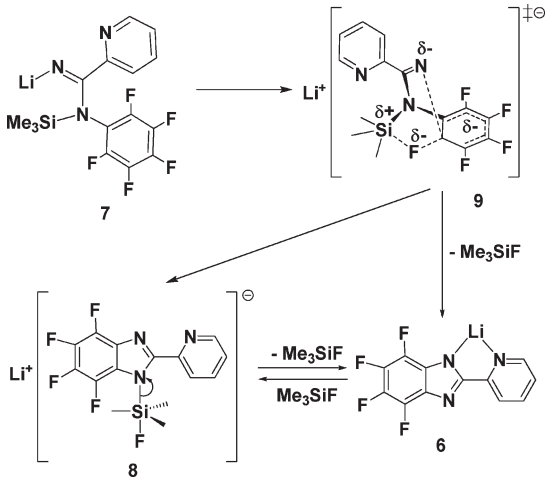

[a] The TMEDA ligand was omitted for clarity.

Conclusions

Lithium *N*-trimethylsilylpentafluoroanilide (**4**) reacts with 2-cyanopyridine under mild conditions to cleanly furnish the lithium tetrafluoro-2-(2-pyridyl) benzimidazolate complex (**6**) and Me_3SiF. *N*-trimethylsilyl-*N*′-pentafluorophenyl-2-pyridylamidinate (**5**) can be isolated as a dormant intermediate from the reaction mixture at low temperatures. The solid state structures of the anilide and the amidinate possess some interesting properties such as C−F→Li interaction in the former and delocalization of electron density from the κ^1-*Z*-*syn* coordinated amidinate core to silicon. The solid state structure of these compounds corroborated by ^{1}H, ^{19}F, and ^{13}C NMR spectroscopy indicates that a silicon-assisted nucleophilic aromatic substitution is probably the main operative mechanism for the facile cyclization reaction which presumably occurs via the hypervalent silicate complex **8**.

Experimental Section

General Procedures. All manipulations of air-sensitive materials were carried out with the vigorous exclusion of oxygen and moisture in an oven-dried or flamed Schlenk-type glassware on a dual-manifold Schlenk line, or interfaced to a high vacuum (10^{-5} Torr) line, or in a nitrogen-filled Vacuum Atmospheres glovebox with a medium-capacity recirculator (1−2 ppm O_2). Argon and nitrogen were purified by passage through a MnO oxygen-removal column and a Davison 4 Å molecular sieve column. Analytically pure solvents were distilled under nitrogen from potassium benzophenone ketyl (THF), Na (toluene, TMEDA), and Na/K alloy (ether, hexane, toluene-d_8, THF-d_8). *N*-trimethylsilylpentafluoroaniline (**1**) was prepared as in the literature.[48] TMSF was prepared by the cyclization reaction of complex **5** (vide infra). The reaction vessel was interfaced to a gentle stream of nitrogen which carried the emitted TMSF through a cooled Schlenk flask (−30 °C). The liquefied TMSF was further purified by distillation at room temperature. *n*-butyllithium (1.6 M in hexane) and 2-cyanopyridine were purchased from Aldrich and used as received.

NMR spectra were recorded on Bruker Avance 300 and 500 spectrometers. ^{1}H and ^{13}C Chemical shifts are referenced to internal solvent resonances and reported relative to tetramethylsilane. ^{19}F, ^{7}Li, and ^{29}Si chemical shifts were referenced according

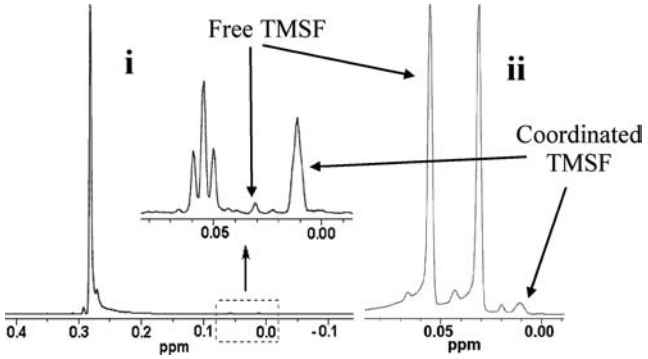

Figure 6. ^{1}H NMR monitoring of intermediates in the cyclization reaction. (i) TMS region in the ^{1}H NMR spectrum of complex **5**. The large singlet at 0.287 ppm belongs to complex **5**. In the enlarged small box area, the triplet at 0.055 ppm with J_{H-F} = 1.4 Hz belongs to the imide **7**, the broad signal at 0.011 ppm probably relates to the silicate complex **8**, and the smallest signal at 0.031 ppm relates to uncoordinated TMSF (compare to (ii) herein). (ii) TMS region in the ^{1}H NMR spectrum of complex **6** with added TMSF. The large doublet (0.031−0.056 ppm) belongs to uncoordinated TMSF, and the broad signal at 0.011 ppm relates to the silicate complex **8**.

to the IUPAC recommendations.[64] The experiments were conducted in Teflon-sealed NMR tubes (J. Young) after preparation of the sample under anaerobic conditions, with dried toluene-d_8 or THF-d_8.

X-ray Crystallographic Measurements. The single crystalline material was immersed in Parathone-N oil and was quickly fished with a capillary tube and mounted on the Kappa CCD diffractometer under a cold stream of nitrogen at 200 K. Data collection was performed using monochromatized Mo Kα radiation using omega scans and phi scans to cover the Ewald sphere.[65] Accurate cell parameters were obtained with the amount of indicated reflections (Table 1).[66] The structure was solved by SHELXS97 direct methods,[67] and refined by SHELXL97 program package.[68] The atoms were refined anisotropically. Hydrogens were included using the riding mode. Software used for molecular graphics: ORTEP, TEXRAY Structure Analysis package[69] Cell parameters and refinement data is presented in Table 1.

Synthesis of $(Me_3SiNC_6F_5)Li\cdot 2THF$ (2). A 2.015 gr portion (7.7 mmol) of complex **3** was weighed into a Schlenk flask, which was cooled to liquid nitrogen temperature and pumped-down. About 20 mL of THF was vacuum-transferred into the flask, which was then placed in a bath of acetone at −70 °C. The flask was filled with argon, and the stirring began. The bath was allowed to reach room temperature, yielding a yellow solution.

Caution! *When the addition of THF to complex **3** is performed at room temperature, a vigorous exothermic reaction occurs, accompanied with combustion.*

^{1}H NMR (300 MHz, THF d_8): δ = 3.579 (s, OC*H*D), 1.725 (s, OCD_2CHD) 0.038 (t, J_{H-F} = 1.3 Hz, 9H, CH_3Si); ^{19}F NMR (282 MHz, THF d_8): δ = −171.40 (t, $^{3}J_{FF}$ = 16.0 Hz, 2F, *o*-F), −176.18 (t, $^{3}J_{FF}$ = 21.0 Hz, 2F, *m*-F), −196.68 (m, 1F, *p*-F); ^{13}C NMR (76.5 MHz, THF d_8): δ = 143.09 (m, $^{1}J_{CF}$ = 223.4 Hz, 1C, *p*-C-F), 139.53 (m, $^{1}J_{CF}$ = 236.0 Hz, 2C, *m*-C-F), 137.48 (m, 1C, C−N), 127.36 (m, $^{1}J_{CF}$ = 230.0 Hz, 2C, *o*-C-F), 67.43 (q, OCD_2CD_2), 25.32 (q, OCD_2CD_2), 3.08 (t, J_{CF} = 3.4 Hz, 3C, CH_3Si); ^{7}Li NMR (194.4 MHz, toluene d8): δ = 0.888; ^{29}Si NMR (99.3 MHz, toluene d8): δ = −11.067.

Synthesis of $[(Me_3SiNC_6F_5)Li]_n$ (3). A Swivel frit equipped with two 250 mL flasks was charged with 7.050 gr (27.6 mmol) of the aniline **1** inside the glovebox. The frit was then connected to a high vacuum line and 90 mL of hexane were added. The resulting solution was cooled to −50 °C and 19.0 mL (30.4 mmol, 1.10 equiv) of 1.6 M solution of ^{n}BuLi in hexane was added dropwise using a syringe. The cooling bath was removed, and the mixture was allowed to reach room temperature and was kept stirring for an additional hour. The white precipitate was decanted and washed twice with 50 mL of hexane (6.705 gr, 93.0% yield). Decomposition is noted above 58 °C. Anal. Calcd for $C_9H_9F_5LiNSi$ (261.19): C, 41.39; H, 3.47; F, 36.37; N, 5.36. Found: C, 40.93; H, 3.76; F, 33.07; N, 4.95.

Synthesis of $(Me_3SiNC_6F_5)Li\cdot TMEDA$ (4). A Swivel frit equipped with two 100 mL flasks was charged with 3.869 gr (14.8 mmol) of the anilide **3** inside the glovebox. The frit was then connected to a high vacuum line, and 30 mL of toluene were added. The resulting suspension was cooled to 0 °C, and 5.0 mL (15.4 mmol, 1.04 equiv) of TMEDA were added, giving an almost clear yellow-tan solution, which was stirred for an additional hour and filtered to remove solid impurities. Volatiles were gradually evaporated from the filtrate until precipitation started, and the concentrated solution was kept at −50 °C overnight to yield faint-yellow crystals of the product. The crystals were separated from the mother liquor by decantation, washed twice with small amount of cold hexane and dried under vacuum (4.774 gr, 85.5% yield). Decomposition is noted above 71 °C. ^{1}H NMR (300 MHz, Toluene d_8): δ = 1.695 (s, 12H, CH_3N), 1.568 (s, 4H, CH_2N), 0.355 (t, J_{HF} = 1.4 Hz, 9H, CH_3Si); ^{19}F NMR (282 MHz, toluene d_8): δ = −170.653 (m, 2F, o-F), −173.845 (t, $^{3}J_{FF}$ = 24.3 Hz, 2F, m-F), −193.799 (m, 1F, p-F); ^{13}C NMR (76.5 MHz, toluene d_8): δ = 142.5 (m, $^{1}J_{CF}$ = 240.3 Hz, 1C, *p*-C-F), 139.6 (m, $^{1}J_{CF}$ = 251.8 Hz, 2C, *m*-C-F), 137.0 (t, $^{2}J_{CF}$ = 15.9 Hz,1C, C−N), 56.3 (s, 2C, CH_2N), 45.1 (s, 4C, CH_3N), 3.6 (t, J_{CF} = 3.2 Hz, 3C, CH_3Si); ^{7}Li NMR (194 MHz, toluene d8): δ = 1.4168; ^{29}Si NMR (99 MHz, toluene d8): δ = −8.4680. Anal. Calcd for $C_{15}H_{25}F_5LiN_3Si$ (377.40): C, 47.74; H, 6.68; F, 25.17; N, 11.13. Found: C, 46.25; H, 6.58; F, 25.62; N, 10.48.

Synthesis of $[C_6F_5NC(2\text{-}C_5H_4N)NSiMe_3]Li\cdot TMEDA$ (5). A 3.925 gr portion (10.4 mmol) of complex **4** was charged in the glovebox into a Swivel frit equipped with two 100 mL flasks. The frit was connected to a high vacuum line, and 40 mL of toluene were added. The resulted solution was cooled to −10 °C and 1.0 mL (10.4 mmol) of 2-cyanopyridine was added dropwise using a syringe. The cooling bath was removed, and the mixture was stirred at room temperature for 2 h, after which a clear olive-brown solution was obtained. The solution was filtered to remove solid impurities, and volatiles were evaporated from the filtrate until precipitation started. The concentrated solution was stirred at −50 °C for 30 min, and the light-brown precipitate was allowed to settle. The top liquid was carefully decanted, and the precipitate was washed with a small amount of cold hexane. This purification stage was repeated with another batch (ca. 20 mL) of toluene, to give 4.171 gr (83.3% yield) of the amidinate **5**. Slow evaporation of toluene (over 3 h) from a saturated solution of **5** afforded X-ray quality olive-brown crystals of 5. Decomposition is noted above 60 °C. ^{1}H NMR (300 MHz, Toluene d_8): δ = 8.657 (d, ^{3}J = 8.1 Hz, 1H, py-H_6), 7.715 (d, ^{3}J = 4.8 Hz, 1H, py-H_3), 7.220 (t, ^{3}J = 7.8 Hz, 1H, py-H_4), 6.746 (t, ^{3}J = 4.8 Hz, 1H, py-H_5), 1.709 (s, 12H, CH_3N), 1.682 (s, 4H, CH_2N), 0.287 (s, 9H, CH_3Si); ^{19}F NMR (282 MHz, toluene d_8): δ = −153.857 (br s, 2F, o-F), −171.797 (t, $^{3}J_{FF}$ = 22.8 Hz, 2F, m-F), −176.032 (br s, 1F, p-F); ^{13}C NMR (76.5 MHz, toluene d_8): δ = 161.027 (s, 1C, N···C···N),

(64) Harris, R. K.; Becker, E. D.; Cabral De Menezes, S. M.; Goodfellow, R.; Granger, P. *Pure Appl. Chem.* **2001**, *73*, 1795–1818.
(65) *Kappa CCD Server Software*; Nonius BV: Delft, The Netherlands, **1997**.
(66) Otwinowski, Z.; Minor, W. *Methods Enzymol.* **1997**, *276*, 307–326.
(67) Sheldrick, G. M. *Acta Crystallogr., Sect. A: Found. Crystallogr.* **1990**, *A46*, 467–473.
(68) Sheldrick, G. M. *SHELXL97, Program for the Refinement of Crystal Structures*; University of Gottingen: Gottingen, Germany, **1997**.
(69) *ORTEP, TEXRAY Structure Analysis Package*; Molecular Structure Corporation, MSC: 3200 Research Forest Drive, The Woodlands, TX, **1999**.

147.169 (s, 1C, py-C_2), 145.308 (s, 1C, py-C_6), 143.08, (m, $^1J_{CF}$ = 238.9, 2C, *o*-C-F), 139.14 (m, 2C, *m*-C-F), 133.37 (m, 1C, C−N), 130.88 (m, 1C, *p*-C-F), 137.122 (s, 1C, py-C_4), 125.286 (s, 1C, py-C_5), 123.032 (s, 1C, py-C_3), 56.471 (CH_2N), 44.901 (CH_3N), 3.165 (CH_3Si). ^{7}Li NMR (194.4 MHz, toluene d_8): δ = 2.2899; ^{29}Si NMR (59.6 MHz, toluene d_8): δ = −21.301. Anal. Calcd for $C_{21}H_{29}F_5LiN_5Si$ (481.51): C, 52.38; H, 6.07; F, 19.73; N, 14.54. Found: C, 49.09; H, 5.79; F, 21.28; N, 12.71.

Synthesis of [$C_6F_4N_2C$(2-C_5H_4N)]Li·TMEDA (6). A 2.000 gr portion (5.1 mmol) of complex **5** was charged in the glovebox into a Swivel frit equipped with two 100 mL flasks. The frit was interfaced to a high vacuum line with the bubbler connected to a well-ventilated fume-hood, and 20 mL of toluene were added. The resulted solution was heated to 50 °C and kept at this temperature for 10 min, during which massive bubbling of TMSF occurs. The heating bath was removed, and the gray suspension was allowed to reach room temperature. The volume of the reaction mixture was reduced to about half by vacuum, and 20 mL of hexane were added. The resulted suspension was cooled to −30 °C and filtered. The gray solid was washed with 20 mL of cold hexane after which its color brightened to off-white. (1.878 gr, 94.6% yield), mp 170 °C (dec.). ^{1}H NMR (300 MHz, Toluene d_8): δ = 8.674 (d, ^3J = 8.4 Hz, 1H, py-H_6), 7.749 (d, ^3J = 2.7 Hz, 1H, py-H_3), 7.142 (t, ^3J = 4.5 Hz, 1H, py-H_4), 6.621 (t, ^3J = 8.1 Hz, 1H, py-H_5), 1.930 (s, 12H, CH_3N), 1.799 (s, 4H, CH_2N); ^{1}H NMR (300 MHz, THF d_8): δ = 8.490 (m, ^3J = 1H, py-H_6), 8.471 (m, 1H, py-H_3), 7.864 (t, ^3J = 8.1 Hz, 1H, py-H_5), 6.621 (t, ^3J = 4.92 Hz, 1H, py-H_4), 3.582 (s, OC*H*D), 2.353 (s, 4H, CH_2N), 2.174 (s, 12H, CH_3N), 1.725 (s, OCD_2CHD); ^{19}F NMR (282 MHz, toluene d_8): δ = −160.640 (br s, 1F, F_7), −164.788 (br s, 1F, F_4), −176.518 (br s, 1F, F_6), −177.205 (br s, 1F, F_5) ; ^{19}F NMR (282 MHz, THF d_8): δ = −164.837 (br s, 2F, o-F), −179.712 (br s, 2F, m-F); ^{7}Li NMR (194.4 MHz, toluene d8): δ = 2.7509; ^{13}C NMR (76.5 MHz, THF d_8): δ = 162.68 (s, 1C, N···C···N), 155.59 (s, 1C, py-C_2), 148.85 (s, 1C, py-C_6), 138.91 (s, 1C, py-C_4), 138.36 (m, $^1J_{CF}$ = 246.4 Hz, 2C, *o*-C-F), 135.78 (m, $^1J_{CF}$ = 237.9 Hz, 2C, *m*-C-F), 133.53 (m, 2C, C−N), 123.76 (s, 1C, py-C_5), 122.69 (s, 1C, py-C_3), 67.42 (q, OCD_2CD_2), 58.76 (s, 2C, CH_2N), 46.14 (s, 4C, CH_3N), 25.32 (q, OCD_2CD_2). Anal. Calcd for $C_{18}H_{20}F_4LiN_5$ (389.32): C, 55.53; H, 5.18; F, 19.52; N, 17.99. Found: C, 52.08; H, 4.75; F, 21.62; N, 16.32.

Acknowledgment. This research was supported by the U.S.A.-Israel Binational Science Foundation under contract 2004075. S.A. thanks Mr. Raymond Rosen for the fellowship.

Supporting Information Available: X-ray crystallographic data in CIF files for compounds **4**−**6**. This material is available free of charge via the Internet at http://pubs.acs.org.